INTERNATIONAL JOURNAL OF AGRICULTURE & BIOLOGY
ISSN Print: 1560–8530; ISSN Online: 1814–9596
25–950/2026/35:350301
http://www.fspublishers.org

Full Length Article

Phytochemical Insights into Plantation Timber: Cudracusisoflavone and Bioactivities of *Eucalyptus pellita* Leaf Extracts from North Sumatran Clones

Murni Suryani Lumbantoruan, Sovia Lenny* and Helmina Br Sembiring
Department of Chemistry, Faculty of Mathematics and Natural Sciences, Universitas Sumatera Utara, Medan 20155, North Sumatra, Indonesia
*For correspondence: sofia1@usu.ac.id
Received 08 September 2025; Accepted 17 December 2025; Published online 11 February 2026

Editor: Khawar Jabran

Abstract

Eucalyptus pellita F. Muell., a high-yielding timber species commercially planted in many clonal plantations in North Sumatra, Indonesia has been exploited only for its wood, but the leaf biomasses are relatively understudied for their bioactivity. The aim of this study was to investigate the potential secondary metabolites in *E. pellita* leaf extracts to support its future utilization other than timber production. Crude extracts were obtained by maceration technique using ethyl acetate, hexane, and methanol then each fraction was analyzed for phytochemical contents (phenolics, flavonoids), total antioxidant capacity, antioxidant activity (2,2-diphenyl-1-picrylhydrazyl/DPPH radical scavenging) and antibacterial activity against *Bacillus subtilis*, *Escherichia coli* and *Staphylococcus aureus*. Compounds were isolated and purified using column chromatography and preparative thin-layer chromatography (TLC), following their structural elucidation and characterization based on UV-Vis, FT-IR, and ^{1}H-NMR outputs. The ethyl acetate fraction among the fractions revealed the highest phenolic (205.2 mg GAE/g of extract) and flavonoid (44.7 mg QE/g of extract) contents and strongest antioxidant activity (IC_{50} = 62.55 μg/mL). The n-hexane fraction produced the largest inhibition zones (15.5–19.2 mm), followed by the ethyl acetate fraction (14.8–15.1 mm) and the methanolic fraction (10.1–13.2 mm) against the tested bacteria. Structural analysis resulted in the identification of cudracusisoflavone, an isoflavone, as the major compound in the ethyl acetate fraction. These findings promote the use of *E. pellita* leaves as a rich source of bioactive phytochemicals, especially cudracusisoflavone which can be utilized for drug development.

Keywords: Cudracusisoflavone; *Eucalyptus*; Flavonoids; Non-timber Forest Products; Pharmaceuticals

Introduction

Industrial plantation forests form a crucial component of Indonesia's forest sector, covering 7.2 million hectares (ha), of which 4.01 million ha are on Sumatra Island and 2.77 million ha on Borneo, and the remaining ones are dispersed in the Moluccas, and Nusa Tenggara, Papua, and Sulawesi. These plantations are the main source of raw material for the paper and pulp industries, which contribute significantly to the national economy in terms of both gross domestic product and employment opportunities. In the year 2020, industrial plantation forests produced around 45 million m^3 of wood with over 99% coming from *Acacia* and *Eucalyptus* species (Lelana *et al.* 2022; Ali *et al.* 2024). Globally, plantation forests have come to rely on a limited number of fast-growing tree species, for example *Acacia* and *Eucalyptus* that have been widely recognized in the tropics (Nambiar *et al*. 2018). *Eucalyptus* spp. (*Myrtaceae*) is a genus of indigenous plant species from Australia and Tasmania that are widely introduced and cultivated nowadays in many countries because of its adaptability and rapid growth (Nirsatmanto *et al.* 2023). Recently, nine species (*Eucalyptus camaldulensis, Eucalyptus dunnii, Eucalyptus. globulus, Eucalyptus grandis, Eucalyptus nitens, Eucalyptus pellita, Eucalyptus saligna, Eucalyptus tereticornis, Eucalyptus urophylla* and their hybrids) dominate global *Eucalyptus* plantations and account for over 90% of total cultivation (Pirralho *et al.* 2014). Besides their silvicultural use, some *Eucalyptus* species contained essential oils and diverse secondary metabolites with a broad spectrum of pharmacological activities such as antifungal, antimicrobial, antioxidant, wound healing, and others (Chu *et al.* 2014; Chandorkar *et al.* 2021; Purwoko *et al.* 2024). In Indonesia, *Eucalyptus pellita* F. Muell. has

To cite this paper: Lumbantoruan MS, S Lenny, HB Sembiring (2026). Phytochemical insights into plantation timber: Cudracusisoflavone and bioactivities of *Eucalyptus pellita* leaf extracts from North Sumatran Clones. *Intl J Agric Biol* 35:350301. https://doi.org/10.17957/IJAB/15.2446
© 2026 The Authors. International Journal of Agriculture and Biology published by Friends Science Publishers, Faisalabad, Pakistan
This is an open access article under the terms of the Creative Commons Attribution License, which permits non-commercial use, distribution and reproduction in any medium, provided the original work is properly cited

been cultivated to produce pulpwood intensively. The private company, Toba Pulp Lestari, maintains large-scale clonal plantations of *E. pellita* in 12 regencies of North Sumatra, between altitudes of 1,154 and 1,365 meters above sea level (masl), where superior clones have been planted for timber production (Purwoko *et al.* 2024). Its non-wood potential, particularly its leaves, has not yet fully been utilized although it's economic value as a source of wood. Leaf mass, most often abandoned or composted, contains phenolic substances and essential oils that are potentially an untapped reservoir of bioactive metabolites (Puig *et al*. 2013; Lenny *et al.* 2021). To optimize the economic value of plantation forests, the Indonesian government has enforced each plantation sector to adopt the integrated forest management systems which combine timber production and non-timber forest products (NTFPs), as mandated by the Ministry of Environment and Forestry Regulation No. 8/2021 (Atinga and Bannor 2024). This study aimed to investigate the phytochemical content of *E. pellita* leaves, focusing on their antioxidant and antibacterial properties. Stepwise solvent fractionation, followed by chemical profiling and structural characterization of the major compounds, was conducted to identify a signature phytochemical from *E. pellita*, a North Sumatran clone.

Materials and Methods

Materials

All chemicals used in this study were of analytical grade and were used without further purification. TLC was carried out on silica gel 60 F254 plates (Merck). Additional chemicals and solvents were obtained from Sigma-Aldrich. UV-Vis spectra were recorded using a Varian Cary 100 Conc spectrophotometer to determine the λ_{max}. Functional groups of phenolic compounds were characterized by FT-IR spectroscopy using a Shimadzu Prestige system. ^{1}H-NMR spectra were acquired on an Agilent spectrometer operating at 500 MHz and 125 MHz, respectively. Samples were prepared in CD_3OD (99.99% purity), with tetramethylsilane (TMS, 99.999% purity) as the internal reference standard. Chemical shifts were reported in δ (mg. kg^{-1}).

Collection of plant materials

Leaf samples of *Eucalyptus pellita* were obtained in March 2023 from an industrial forest plantation managed by Toba Pulp Lestari, in Toba Samosir Regency, North Sumatra Province, Indonesia. The specimen was authenticated by plant taxonomists at the Herbarium MEDA/Medanense, Universitas Sumatera Utara, Medan, Indonesia, under the voucher code No. 099A/MEDA/2023. After collection, the leaves were washed, cut into smaller fragments, sun-dried, and subsequently oven-dried at 45°C. The dried material was further pulverized into a fine powder (1,900 g).

Preparation of plant extracts

A total of 1,900 g of *E. pellita* leaf powder was macerated in 20 L of methanol (MeOH), ensuring complete submersion of the sample. The mixture was allowed to stand for 48 h, after which it was filtered and concentrated using a rotary evaporator to obtain the MeOH extract. This extract was then successively partitioned with n-hexane (C6) until the solvent phase became clear. The remaining MeOH layer was concentrated to remove residual solvent and subsequently extracted with ethyl acetate (EtOAc). The EtOAc fraction was concentrated and evaporated under reduced pressure (*in* v*acuo*) using rotary evaporator to obtain a viscous extract.

Determination of total phenolic content

A 0.5 mL of each fractionated extract was mixed with 0.4 mL of Folin–Ciocalteu reagent (a mixture of phosphomolybdic and phosphotungstic acids). The solution was gently agitated and allowed to react for 4-8 min, followed by the addition of 4.0 mL of 7% sodium carbonate (Na_2CO_3) solution. The solution was thoroughly homogenized and adjusted to a final volume of 10 mL with sterile-distilled water (SDW). It was then incubated at mild temperature (25-28°C) for 2 h, and absorbance was measured at 765 nm using UV-Vis spectrophotometer. Total phenolic content was determined and expressed as milligrams of gallic acid equivalents (GAE) per 100 mg of fresh sample, with each assay performed in triplicate (Ainsworth and Gillespie 2007).

Determination of total flavonoid content

Standard quercetin solutions (2–10 mg. kg^{-1}) and sample solutions (1,000 µg/mL) were prepared. An aliquot of 1.0 mL from each solution was mixed with 3 mL of MeOH, 0.2 mL of 10% $AlCl_3$, and 0.2 mL of 20% anhydrous sodium acetate (CH_3COONa), followed by the addition of 5.6 mL of SDW. The mixtures were homogenized and incubated for 30 min. The absorbance of solution was measured at 440 nm using the same instrument as previously mentioned. Total flavonoid content was determined and expressed as milligrams of quercetin equivalents per 100 mg of fresh sample, with each assay performed in triplicate (Tristantini and Amalia 2019).

Antioxidant assay

Total antioxidant capacity was determined based on the principle of phosphomolybdenum complex formation by Prieto *et al.* (1999). Briefly, a reagent solution containing 4 mM ammonium molybdate, 0.6 *M* sulfuric acid (H_2SO_4), and 28 m*M* sodium phosphate (Na_3PO_4), was mixed with the sample fractions, followed by incubation at 95°C for 90 min in a water bath. After cooling to mild temperature, the

absorbance was measured at 695 nm using the same instrument as previously mentioned. A standard calibration curve was generated using ascorbic acid, and antioxidant activity was expressed relative to this reference. DPPH radical scavenging activity was determined following the method of Marinova and Batchvarov (2011). A methanolic stock solution (1.0 mg/mL) was prepared by dissolving 10 mg of extract in 10 mL of MeOH. From this stock, a 200 μg/mL working solution was prepared by a 1:5 dilution. A series of two-fold dilutions was then performed to obtain the final test concentrations of 100, 50, 25 and 12.5 μg/mL. The DPPH solution (0.3 m*M*) was prepared by dissolving 11.83 mg of DPPH in 100 mL of MeOh and protected from light with aluminum foil. For the assay, 1 mL of the DPPH solution was mixed with 2.5 mL of extract solution, vortexed, and incubated at 37°C for 30 min, following the measurement of its absorbance at 515 nm. The same procedure was applied to ethyl acetate and hexane extracts, with ascorbic acid included as a standard reference. The percentage of DPPH scavenging was calculated using the formula: $[(A_{control} - A_{sample})/A_{control}] \times 100\%$. The half-maximal concentration or IC_{50} values were determined using a four-parameter logistic regression model *via* the AAT Bioquest online calculator (https://www.aatbio.com/tools/ic50-calculator).

Antibacterial test

The antibacterial activity of *E. pellita* fractions was tested against common human pathogenic bacteria such as *Bacillus subtilis*, *Escherichia coli* and *Staphylococcus aureus*, using the disc diffusion method (Balouiri *et al.* 2016). Fractions of C6, EtOAc and MeOH were dissolved in 0.5% (v/v) dimethyl sulfoxide (DMSO) in SDW to achieve a concentration of 400 μg of extract per disc. Bacterial suspensions were standardized to an OD_{600} of 0.08–0.10 and uniformly spread onto Mueller-Hinton Agar (MHA) plates using sterile cotton swabs to produce a bacterial lawn. Sterile filter paper discs loaded with each fraction were placed on the agar surface, followed by incubation at 37°C for 24 h. Chloramphenicol discs (Oxoid, 30 μg) were used as the positive control in the antibacterial assay. Antibacterial activity was indicated by the presence of halo or inhibition zone and measured for its diameters (mm) around the discs using a digital caliper.

Fractionation and purification of major compound in the *E. pellita* leaf extract

Thin-layer chromatography (TLC) analysis was performed on ethyl acetate extract using silica gel 60 GF254 as the stationary phase to determine the optimal solvent system for column chromatography. The mobile phases consisted of solvent mixtures of chloroform ($CHCl_3$) and MeOH in ratios of 90:10, 80:20, 70:30 and 60:40 (v/v). The TLC plates were spotted with the concentrated extract, eluted in a pre-saturated chamber, and visualized using 5% $FeCl_3$. The Rf values were recorded to select the most suitable solvent ratio. For column chromatography, silica gel 60 (70–230 mesh) served as the stationary phase. The EtOAc extract was mixed with silica gel and loaded onto the column. Elution was initiated with 100% $CHCl_3$, followed by stepwise increases in polarity using $CHCl_3$-MeOH mixtures (90:10 to 60:40 v/v). Fractions were collected in 10 mL volumes, analyzed by TLC, and combined based on matching Rf values. The pooled fractions were further concentrated to a paste and subjected to additional TLC analysis to confirm purity. Preparative TLC was prepared using $CHCl_3$: EtOAc (80:20 v/v) as the mobile phase. The paste was spotted onto the TLC plate, eluted, and visualized under UV light. Separated zones were marked, eluted with MeOH : EtOAc (1:1 v/v), and concentrated to obtain a yellow amorphous solid. Final purification was achieved using acetone and n-hexane, yielding a pure compound (10 mg per 0.95 g of crude fraction) confirmed by single TLC spots, UV absorption and a positive reaction with 5% $FeCl_3$. The purified compound was then subjected to UV-Vis, FT-IR and ^{1}H-NMR for structural elucidation and characterization.

Data analysis

Each experiment was carried out in triplicate, and data are expressed as mean ± standard deviation (SD). All multiple-comparison analyses following one-way ANOVA were conducted using Tukey's HSD test to determine pairwise differences among groups with a significance threshold of $P < 0.05$. Statistical analyses were conducted using Minitab® Statistical Software v. 19.0.

Results

The phytochemical and biological properties of the *E. pellita* fractions were evaluated. Quantification of total phenolic and flavonoid contents among fractionated extracts showed significant differences among fractions in both phenolic ($F_{2,6} = 62.39$, $P < 0.001$) and flavonoid ($F_{2,6} = 19.93$, $P < 0.05$) concentrations as presented in Table 1. The EtOAc fraction contained the highest concentrations (205.2 mg GAE/g plant material; 44.7 mg QE/g extract), followed by MeOH, whereas C6 consistently yielded the lowest values. Antioxidant activity, indicated through both TAC and the DPPH radical scavenging activity (Table 2), showed a different pattern. The parameter, TAC was the greatest in MeOH, followed by C6 and EtOAc, although these differences were not significant ($F_{2,6} = 1.71$, $P = 0.259$). However, the EtOAc fraction produced the strongest DPPH scavenging effect, as indicated by the lowest IC_{50} (62.55 μg/mL), with MeOH and C6 demonstrating weaker activity. The discrepancy between the TAC and DPPH results reflects the distinct chemical profiles highlighted by each assay. The MeOH extract might contain the highest

Table 1: Total phenolic and flavonoid content of different *E. pellita* leaf extracts

Fraction(s)	TPC (mg GAE/g of extract)	TFC (mg QE/g of extract)
C6	11.6 ± 9.68 [a]	8.3 ± 10.30 [a]
EtOAc	205.2 ± 33.53 [b]	44.7 ± 4.38 [b]
MeOH	28.31 ± 19.51 [a]	35.0 ± 5.92 [b]

C6 = *n*-hexane; EtOAc = ethyl acetate; MeOH = methanol; TPC = total phenolic content; TFC = total flavonoid content; GAE = gallic acid equivalent; QE = quercetin equivalent. Data are presented in mean ± SD (n = 3). Values with different superscript letters ([a, b]) denote significant difference based on one-way ANOVA test at 95%

Table 2: Total antioxidant activity (TAC) and half-maximal concentration of DPPH scavenging activity (IC_{50}) of different *E. pellita* leaf extracts

Fraction(s)/Standard	TAC (mg AAE/g of extract)	IC_{50} value (μg/mL)
C6	5.3 ± 0.63 [a]	588.28
EtOAc	5.2 ± 0.75 [a]	62.55
MeOH	6.2 ± 0.77 [a]	559.45
Ascorbic acid	-	8.44

C6 = *n*-hexane; EtOAc = ethyl acetate; MeOH = methanol. Data are presented in mean ± SD (n = 3). Values with same superscript letter ([a]) denote no significant difference based on one-way ANOVA test at 95%

Table 3: Antibacterial activity of different *E. pellita* leaf extracts against pathogenic bacteria

Fraction(s)/ Antibiotics	Diameter zone of inhibition (mm)		
	Bacillus subtilis	*Staphylococcus aureus*	*Escherichia coli*
C6	19.2 ± 1.61 [a, x]	15.5 ± 2.18 [a, x]	16.9 ± 2.00 [a, x]
EtOAc	15.0 ± 0.95 [b, x]	14.8 ± 1.12 [a, x]	15.1 ± 1.71 [a, x]
MeOH	13.2 ± 1.36 [b, x]	12.8 ± 1.06 [a, x]	10.1 ± 1.10 [b, y]
Chloramphenicol	32.7 ± 2.52 [c]	33.7 ± 1.16 [b]	32.0 ± 2.00 [c]

C6 = *n*-hexane; EtOAc = ethyl acetate; MeOH = methanol. Data presented in mean ± SD are calculated from triplicate measures. Differences among fractions and bacterial responses were confirmed by Tukey's HSD test, where superscripts (a, b) denote between-fraction differences and (x, y) indicate variation across bacterial strains

abundance of reducing constituents, including larger polymeric or glycosylated molecules that contribute strongly to TAC values. In contrast, the EtOAc fraction was enriched in compounds that act as highly efficient radical scavengers in the DPPH system, consistent with the purification steps that concentrated antioxidants effective under this specific mechanism. Antibacterial screening using the disc diffusion method (Table 3) also demonstrated significant variability among the fractions ($P < 0.001$) and overall their activity was weaker than that of chloramphenicol as the reference antibiotic (> 30 mm). The fraction, C6 produced the largest inhibition zones against *B. subtilis* (19.2 ± 1.61 mm), *E. coli* (16.9 ± 2.00 mm), and *S. aureus* (15.5 ± 2.18 mm). The EtOAc fraction displayed moderate inhibitory activity (14.8-15.1 mm), while MeOH was least active, particularly against *E. coli* (10.1 ± 1.10 mm). More detailed characterization of major constituents was obtained through spectroscopic analysis of the EtOAc fraction. UV absorbance indicated the presence of conjugated aromatic systems (Fig. 1), FTIR confirmed the presence of hydroxyl, carbonyl, aromatic and ether functional groups (Fig. 2) and ^{1}H-NMR data indicated proton shifts for an isoflavone skeleton with methoxy substitution (Fig. 3; Table 4). Based on these characteristics,

Table 4: Comparison of ^{1}H-NMR data for Cudracusisoflavone with the reported values (Jo *et al.* 2021)

Carbon position	Cudracusisoflavone (δH)	Reported values (δH)
2	8.09 (s)	8.21 (s)
2′	7.71 (d)	7.42 (d)
3′	7.62 (dd)	6.87 (d)
5′	7.62 (dd)	6.87 (d)
6′	7.71 (d)	7.42 (d)
1″	3.51 (d)	3.47 (d)
2″	5.35 (t)	5.26 (t)
4″	1.89 (s)	1.83 (s)
5″	1.61 (s)	1.71 (s)
1‴	5.26 (d)	5.20 (d)
2‴	4.35 (d)	4.50 (d)
4‴	1.40 (s)	1.34 (s)
5‴	1.24 (s)	1.12 (s)
OCH_3	3.81 (s)	3.55 (s)

s = singlet, d = doublet, dd = doublet of doublets

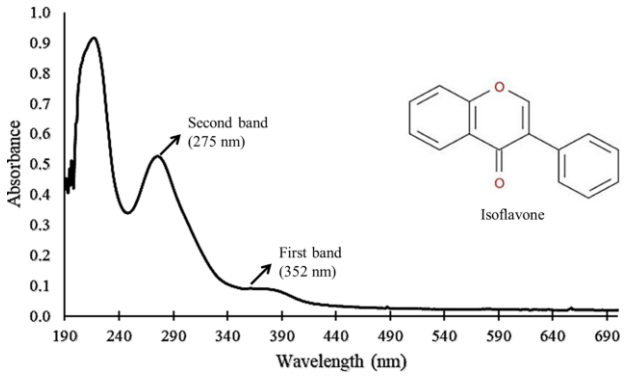

Fig. 1: UV-Vis spectrum of an isolated compound in the *E. pellita* EtOAc leaf extract

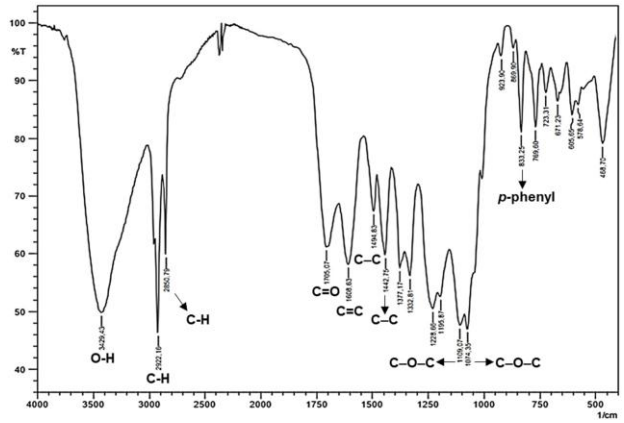

Fig. 2: FT-IR spectrum of an isolated compound in the *E. pellita* EtOAc leaf extract

the compound was identified as cudracusisoflavone, a prenylated isoflavone (Fig. 4).

Discussion

This study initiated the exploration of non-timber forest products from *E. pellita* by evaluating phytochemicals in its

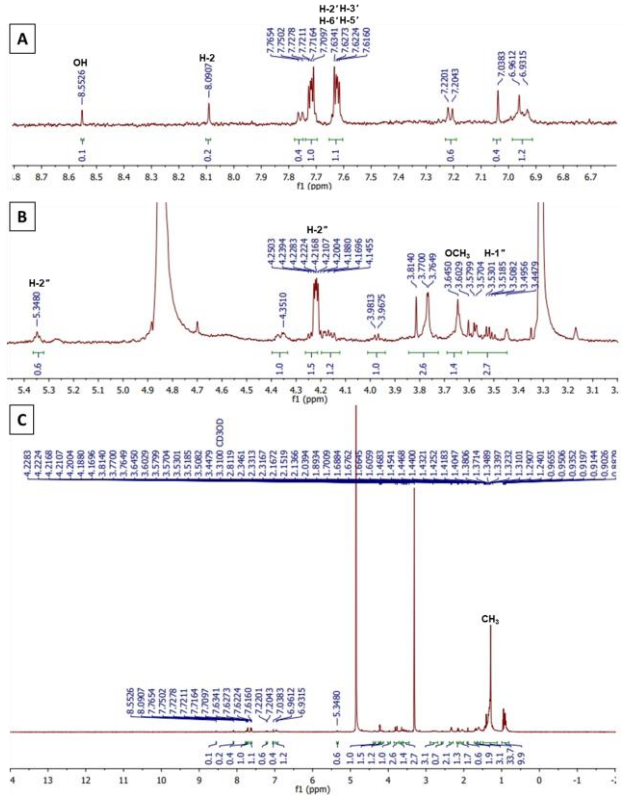

Fig. 3: ^{1}H-NMR spectrum of the isolated compound δH 6.7 - 8.7 mg. kg^{-1} (**A**), δH 3.1 - 5.4 mg. kg^{-1} (**B**), δH 0 - 9 mg. kg^{-1} (**C**) (500 MHz, CD_3OD)

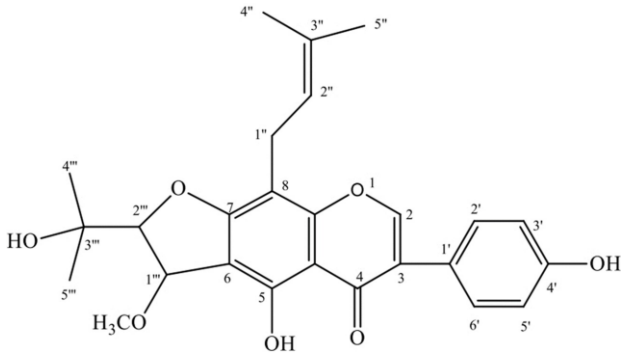

Fig. 4: Chemical structure of cudracusisoflavone

underutilized leaves. While essential oils from related taxa are well studied, other bioactive compounds in this species remain less explored (Proenza *et al.* 2013; Suhardiman and Fitriyana 2023). Among the tested extracts, the EtOAc fraction contained the highest phenolic and flavonoid levels. The total phenolic content of the EtOAc fraction (205.2 mg) was quite similar to other *Eucalyptus* species, such as *E. globulus* leaves (235.87 mg) extracted using 70% EtOH (Dezsi *et al.* 2015) and *E. camaldulensis* seed oils (156.25-167.93 mg) (Olawore and Ololade 2017), but lower than *E. saligna* leaves extracted with pressurized EtOH (618.57 mg GAE/g) (Fischer *et al.* 2020). A similar pattern was observed for flavonoids. The total flavonoid content of the EtOAc fraction (44.7 mg) exceeded that of *E. globulus* leaves (23-35.76 mg), extracted using MeOH or EtOH (Dezsi *et al.* 2015; Sharma *et al.* 2021), yet remained below *E. saligna* (160.27 mg) with pressurized EtOH (Fischer *et al.* 2020). These differences may due to different solvent polarity, with medium-polar solvents such as EtOAc particularly effective in concentrating bioactive metabolites from *E. pellita*. Despite high antioxidant capacity, the EtOAc extract showed weaker antibacterial activity compared to fraction C6. The hexane fraction, although containing the lowest phenolic levels, produced the strongest antibacterial response, indicating that non-polar constituents may contribute to this activity, likely terpenoids. Terpenoid-rich essential oils from various *Eucalyptus* species have shown antibacterial effects, including *E. globulus* against *Listeria monocytogenes* (Dezsi *et al.* 2015), *E. camaldulensis* against *Pseudomonas aeruginosa* and *S. aureus* (Olawore and Ololade 2017) and *E. citriodora* against *E. coli* (Ololade and Olawore 2021). The major compound in the EtOAc fraction of *E. pellita* leaves was characterized using spectroscopic analyses. UV-Vis spectra indicated an isoflavone as the dominant compound, with an absorption peak at 274 nm suggesting conjugated double bonds in an aromatic ring (Dowling *et al.* 2010). Dihydroformononetin, an isoflavonoid derivative, typically shows absorption at 231, 276, and 313 nm, while longer wavelength transitions (320–350 nm) correspond to n→π* transitions, confirming two chromophoric groups (Newberry and Raines 2017). The absorption band at 352 nm, together with FTIR data, further supports the presence of a carbonyl (C = O) group and an aromatic ring. The FTIR spectrum showed a broad O–H stretch at 3429 cm^{-1}, C–O–H bending at 1377 cm^{-1}, and a para-substituted phenyl group at 833 cm^{-1}. The C = O stretching appeared at 1706 cm^{-1}, while aromatic C = C stretches were detected at 1608, 1495, and 1443 cm^{-1}. Ether (C–O–C) stretching bands appeared at 1109 and 1074 cm^{-1}, with aliphatic C–H stretching at 2922 and 2861 cm^{-1}. Additional bands between 1659-1580 cm^{-1} (C=C), 3065 cm^{-1} (aromatic C–H) and 1738 cm^{-1} (C=O) confirmed flavonoid features. The ^{1}H-NMR spectrum (CD_3OD, TMS) revealed aromatic signals between δH 6–8 mg. kg^{-1} (Lenny *et al.* 2013). A singlet at δH 8.09 (H-2, ring A) was characteristic of isoflavones, while ring B showed doublets consistent with a hydroxyl substitution at C-4'. Signals for O–CH_3 appeared as singlets at δH 3.5-4.0 mg. kg^{-1}, with two methoxy groups detected at δH 3.64 (C-1'''). Isopentenyl protons resonated at δH 3.0-3.4 (CH_2), 5.2 (CH) and 1.7-1.8 (CH_3). Additional singlets included δH 1.89 and 1.41 (C-5" and C-4"), δH 1.31 and 0.95 (C-4''' and C-5'''), and δH 8.55 (OH at C-3'''). Furthermore, the ^{1}H-NMR data of cudracus isoflavone were compared with the values reported by Jo *et al.* (2021) to verify the consistency of the proton signals associated with each carbon position (Table 4). The aromatic protons at C-2, C-2′, and C-6′ displayed singlet or doublet patterns similar to those in the reference,

although slight downfield or up field shifts were observed. The protons at C-3′ and C-5′ showed doublet–doublet patterns, but their chemical shifts were higher than those reported previously. Signals assigned to the phenyl side chains, including the methylene and olefinic protons at C-1″, C-2″, C-1‴, and C-2‴, displayed chemical shifts that closely matched the literature, with minimal variation in coupling patterns. The methyl proton signals at C-4″, C-5″, C-4‴, and C-5‴ also appeared as singlets with only minor deviations from the published values. The methoxy group (OCH_3) showed a singlet that was slightly shifted relative to the reference spectrum. Overall, the NMR profile of cudracus isoflavone showed clear consistency with the reported data, reinforcing the structural assignment and confirming that its proton signals align with the established reference values. Cudracusisoflavone and related isoflavones derived from *Cudrania* (*Eucalyptus*) species have been reported to show diverse biological activities, yet their occurrence in *E. pellita* remains largely uncharacterized. Among these compounds, cudraisoflavone A, first isolated from *C. cochinchinensis*, was shown to exert cytotoxic activity against PS cells (Sun *et al.* 1988). Likewise, several isoflavones from the fruits of *C. tricuspidata* demonstrated neuroprotective properties against 6-hydroxydopamine-induced cell death in SH-SY5Y cells (Hiep *et al.* 2015). Cudraisoflavone M, also obtained from *C. cochinchinensis*, exhibited weak cytotoxicity against multiple human cancer cell lines (Wang *et al.* 2017). In addition, prenylated isoflavones from *C. tricuspidata* leaves, including the newly identified cudraisoflavone L, were reported to significantly suppress nitric oxide production in RAW 264.7 macrophages and induce cytotoxicity in HL-60 cells (Anh *et al.* 2017).

Conclusion

The present study confirmed the occurrence of cudracusisoflavone in *Eucalyptus pellita* clones cultivated in North Sumatra by Toba Pulp Lestari and established its structure using UV–Vis, FT-IR and ^{1}H-NMR analyses. Although the compound was successfully isolated, its antioxidant and antibacterial activities were not assessed, and no claims regarding its biological effects can be made at this stage. The findings nonetheless indicate that these clones represent a viable industrial source of phytoconstituents, including cudracusisoflavone. Further investigation into the pharmacological properties of the purified compound is essential to determine its potential as a prospective lead molecule for pharmaceutical development.

Acknowledgments

This project was fully funded by the Directorate of Research, Technology, and Community Service (DRTPM), Ministry of Education, Culture, Research, and Technology (Kemdikbudristek) under the Master's Thesis Research scheme, as stated in the contract: No. 74/UN5.2.3.1/MG. KA-1/KP-DRTPM/B/2023.

Author Contributions

SL and HBS conceptualized and supervised the research. SL developed the methodology. SL and HBS contributed to validation. MSL conducted the investigation, performed the formal analysis, and curated the data. MSL prepared the original draft. SL and HBS reviewed and edited the manuscript. SL acquired the funding.

Conflict of Interest

All authors declare no conflict of interest

Data Availability

Data presented in this study will be available on a personal request to the corresponding author

Ethics Approval

Not applicable to this paper

References

Ainsworth EA, KM Gillepsie (2007). Estimation of total phenolic content and other oxidation substrates in plant tissues using Folin–Ciocalteu reagent. *Nat Prot* 2:875–877

Ali L, R Akhtar, J Hussain, G Khan, S Mumtaz, N Akhtar, R Ali, C Tao (2024). Economic performance of forest plantations in Asian countries. *J Knowl Econ* 15:4997–5017

Anh HLT, DT Tuan, DT Trang, BH Tai, NX Nhiem, PH Yen, PV Kiem, CV Minh, TM Duc, HK Kang, YC Kim, YH Kim (2017). Prenylated isoflavones from *Cudrania tricuspidata* inhibit NO production in RAW 264.7 macrophages and suppress HL-60 cells proliferation. *J Asian Nat Prod Res* 19:510–518

Atinga E, RK Bannor (2024). The commercialisation of NTFPs and conservation of forest: A systematic review for forestry policy. *For Econ Rev* 6:94–121

Balouiri M, M Sadiki, SK Ibnsouda (2016). Methods for *in vitro* evaluating antimicrobial activity: A review. *J Pharm Anal* 6:71–79

Chandorkar N, S Tambe, P Amin, C Madankar (2021). A systematic and comprehensive review on current understanding of the pharmacological actions, molecular mechanisms, and clinical implications of the genus *Eucalyptus*. *Phytomed Plus* 1:100089

Chu C, PE Mortimer, H Wang, Y Wang, X Liu, S Yu (2014). Allelopathic effects of *Eucalyptus* on native and introduced tree species. *For Ecol Manage* 323:79–84

Dezsi Ș, AS Bădărău, C Bischin, DC Vodnar, RS Dumitrescu, AM Gheldiu, A Mocan, L Vlase (2015). Antimicrobial and antioxidant activities and phenolic profile of *Eucalyptus globulus* Labill. and *Corymbia ficifolia* (F. Muell.) K.D. Hill & L.A.S. Johnson leaves. *Molecules* 20:4720–4734

Dowling S, F Regan, H Hughes (2010). The characterisation of structural and antioxidant properties of isoflavone metal chelates. *J Inorg Biochem* 104:1091–1098

Fischer B, EP Gowzdz, G Feltes, P Griep, A Junges, N Paroul, RL Cansian (2020). Antioxidant and antimicrobial properties of *Eucalyptus* leaf extract obtained using pressurized ethanol. *Braz J Dev* 6:74499–74512

Hiep NT, J Kwon, DW Kim, BY Hwang, HJ Lee, W Mar, D Lee (2015). Isoflavones with neuroprotective activities from fruits of *Cudrania tricuspidata*. *Phytochemistry* 111:141–148

Jo YH, S Lee, SW Yeon, A Turk, JH Lee, SM Hong, YK Han, KY Lee, BY Hwang, SY Kim, MK Lee (2021). Anti-diabetic potential of *Masclura tricuspidata* leaves: Prenylated isoflavonoids with α-glucosidase inhibitory and anti-glycation activity. *Bioorg Chem* 114:105098

Lelana NE, S Utami, E Widyati, DM Puspitaningtyas, Yulianti, B Supriadi, S Oktarina, D Priatna (2022). The bacterial composition and diversity in a *Eucalyptus pellita* plantation in South Sumatra, Indonesia. *Diversity* 14:1-14

Lenny S, HB Sembiring, MZE Sinaga (2021). Isolation of phenolic compounds from *Eucalyptus citriodora* leaves. *In: American Institute of Physics Conference Series*, Vol. 2342, p:80005

Lenny S, T Barus, L Marpaung, MP Nasution (2013). Structure elucidation of flavonoid compound from the leaves of *Coleus atropurpureus* Benth using 1D- and 2D-NMR techniques. *Malays J Anal Sci* 17:255–261

Marinova G, V Batchvarov (2011). Evaluation of the methods for determination of the free radical scavenging activity by DPPH. *Bulg J Agric Sci* 17:11–24

Nambiar EKS, CE Harwood, DS Mendham (2018). Paths to sustainable wood supply to the pulp and paper industry in Indonesia after diseases have forced a change of species from acacia to eucalypts. *Aust For* 81:148–161

Newberry RW, RT Raines (2017). The n→π* Interaction. *Acc Chem Res* 50:1838–1846

Nirsatmanto A, S Sunarti, AI Putri, T Herawan, NK Kartikawati, L Haryjanto, F Lestari, A Rimbawanto (2023). *Eucalyptus pellita* and *Acacia* hybrid species: Potential bioenergy plantation in managing the risk of invasive in Indonesia. *In: IOP Conference Series: Earth and Environmental Science*, Vol. 1182, pp:1-11. IOP Publishing

Olawore NO, ZS Ololade (2017). *Eucalyptus camaldulensis* var. Nancy and *Eucalyptus camaldulensis* var. Petford seed essential oils: Phytochemicals and therapeutic potentials. *Chem Sci J* 8:1–6

Ololade ZS, NO Olawore (2021). Health benefits of the fruit essential oil of *Eucalyptus citriodora*: Secondary metabolites, radical scavenging, antioxidant, anti inflammatory, analgesic, antimicrobial potential. *Intl J Drug Discov* 13:1–7

Pirralho M, D Flores, VB Sousa, T Quilho, S Knapic, H Pereira (2014). Evaluation on paper making potential of nine *Eucalyptus* species based on wood anatomical features. *Industr Crops Prod* 54:327–334

Prieto P, M Pineda, M Aguilar (1999). Spectrophotometric quantitation of antioxidant capacity through the formation of a phosphomolybdenum complex: Specific application to the determination of vitamin E1. *Anal Biochem* 269:337–341

Proenza YG, RQ Álvarez, YV Tamayo, MA Saavedra, YS Garcia, RH Espinosa (2013). Chemical composition and antibacterial activity of the essential oil from *Eucalyptus pellita* F. Muell. *J Med Plant Res* 7:1979–1983

Puig CG, L Álvarez-Iglesias, MJ Reigosa, N Pedrol (2013). *Eucalyptus globulus* leaves incorporated as green manure for weed control in maize. *Weed Sci* 61:154–161

Purwoko A, Muhdi, RK Sari, I Azhar, YRU Sianturi, H Sembiring (2024). The assessment of essential oil potential from waste logging of different eucalyptus clones in PT Toba Pulp Lestari Tbk's industrial plantation forests, Indonesia. *Plant Sci Today* 11:681–687

Sharma A, M Chahal, I Kaur (2021). Antioxidant and bioactivities of leaf extracts from *Eucalyptus globulus*. *Arab J Med Aroma Plants* 7:385–406

Suhardiman A, F Fitriyana (2023). The harvested of eucalyptus leaves as sources of essential oil production from timber forest plantation. *In: IOP Conference Series: Earth and Environmental Science*, Vol. 1282, pp:1-7. IOP Publishing

Sun NJ, CJ Chang, JM Cassady (1988). A cytotoxic isoflavone from *Cudrania cochinchinensis*. *Phytochemistry* 27:951–952

Tristantini D, R Amalia (2019). Quercetin concentration and total flavonoid content of anti atherosclerotic herbs using aluminum chloride colorimetric assay. *In: AIP Conference Proceedings*, Vol. 2193, pp:1-8. AIP Publishing LLC

Wang LX, HR Zheng, FC Ren, TG Chen, XM Li, XJ Jiang, F Wang (2017). Polysubstituted isoflavonoids from *Spatholobus suberectus*, *Flemingia macrophylla*, and *Cudrania cochinchinensis*. *Nat Prod Bioprosp* 7:201–206